

GROWTH on GW190425: Searching thousands of square degrees to identify an optical or infrared counterpart to a binary neutron star merger with the Zwicky Transient Facility and Palomar Gattini IR

MICHAEL W. COUGHLIN,¹ TOMÁS AHUMADA,² SHREYA ANAND,¹ KISHALAY DE,¹ MATTHEW J. HANKINS,¹ MANSI M. KASLIWAL,¹ LEO P. SINGER,^{3,4} ERIC C. BELL,⁵ IGOR ANDREONI,¹ S. BRADLEY CENKO,^{3,4} JEFF COOKE,^{6,7} CHRISTOPHER M. COPPERWHEAT,⁸ ALISON M. DUGAS,¹ JACOB E. JENCSION,¹ DANIEL A. PERLEY,⁸ PO-CHIEH YU,⁹ VARUN BHALERAO,¹⁰ HARSH KUMAR,¹⁰ JOSHUA S. BLOOM,¹¹ G.C. ANUPAMA,¹² MICHAEL C. B. ASHLEY,¹³ ASHOT BAGDASARYAN,¹ RAHUL BISWAS,¹⁴ DAVID A. H. BUCKLEY,^{15,16} KEVIN B. BURDGE,¹ DAVID O. COOK,¹⁷ JOHN CROMER,¹⁸ VIRGINIA CUNNINGHAM,² ANTONINO D'AÍ,¹⁹ RICHARD G. DEKANY,¹⁸ ALEXANDRE DELACROIX,¹⁸ SIMONE DICHIARA,^{3,2} DMITRY A. DUEV,¹ ANIRBAN DUTTA,¹² MICHAEL FEENEY,¹⁸ SARA FREDERICK,² PRADIP GATKINE,² SHAON GHOSH,²⁰ DANIEL A. GOLDSTEIN,¹ V. ZACH GOLKHOU,^{5,21,*} ARIEL GOOBAR,¹⁴ MATTHEW J. GRAHAM,¹ HIDEKAZU HANAYAMA,²² TAKASHI HORIUCHI,²² TIARA HUNG,²³ SAURABH W. JHA,^{24,25} ALBERT K. H. KONG,²⁶ MATTEO GIOMI,²⁷ DAVID L. KAPLAN,²⁰ V. R. KARAMBELKAR,¹⁰ MAREK KOWALSKI,^{28,29} SHRINIVAS R. KULKARNI,¹ THOMAS KUPFER,³⁰ VALENTINA LA PAROLA,¹⁹ FRANK J. MASCI,¹⁷ PAOLO MAZZALI,⁸ ANNA M. MOORE,³¹ MOSES MOGOTSI,^{16,15} JAMES D. NEILL,¹ CHOW-CHOONG NGEOW,⁹ JORGE MARTÍNEZ-PALOMERA,³² M. PAVANA,¹² ERAN O. OFEK,³³ ATHARVA SUNIL PATIL,⁹ REED RIDDLE,¹⁸ MICKAEL RIGAULT,³⁴ BEN RUSHOLME,¹⁷ EUGENE SERABYN,³⁵ DAVID L. SHUPE,¹⁷ YASHVI SHARMA,¹⁰ JESPER SOLLERMAN,³⁶ JAMIE SOON,³¹ KAI STAATS,³⁷ KIRSTY TAGGART,⁸ HANJIE TAN,⁹ TONY TRAVOUILLOON,³¹ ELEONORA TROJA,^{2,3} GAURAV WARATKAR,¹⁰ AND YOICHI YATSU³⁸

¹Division of Physics, Mathematics, and Astronomy, California Institute of Technology, Pasadena, CA 91125, USA

²Department of Astronomy, University of Maryland, College Park, MD 20742, USA

³Astrophysics Science Division, NASA Goddard Space Flight Center, MC 661, Greenbelt, MD 20771, USA

⁴Joint Space-Science Institute, University of Maryland, College Park, MD 20742, USA

⁵DIRAC Institute, Department of Astronomy, University of Washington, 3910 15th Avenue NE, Seattle, WA 98195, USA

⁶Australian Research Council Centre of Excellence for Gravitational Wave Discovery (OzGrav), Swinburne University of Technology, Hawthorn, VIC, 3122, Australia

⁷Centre for Astrophysics and Supercomputing, Swinburne University of Technology, Hawthorn, VIC, 3122, Australia

⁸Astrophysics Research Institute, Liverpool John Moores University,

IC2, Liverpool Science Park, 146 Brownlow Hill, Liverpool L3 5RF, UK

⁹Graduate Institute of Astronomy, National Central University, 32001, Taiwan

¹⁰Indian Institute of Technology Bombay, Powai, Mumbai 400076, India

¹¹Department of Astronomy, University of California, Berkeley, CA 94720-3411, USA; Physics, Lawrence Berkeley National Laboratory, 1 Cyclotron Road, MS 50B-4206, Berkeley, CA 94720, USA

¹²Indian Institute of Astrophysics, II Block Koramangala, Bengaluru 560034, India

¹³School of Physics, University of New South Wales, Sydney NSW 2052, Australia

¹⁴The Oskar Klein Centre, Department of Physics, Stockholm University, AlbaNova, SE-106 91 Stockholm, Sweden

¹⁵South African Astronomical Observatory, P.O. Box 9, Observatory 7935, Cape Town, South Africa

¹⁶Southern African Large Telescope Foundation, P.O. Box 9, Observatory 7935, Cape Town, South Africa

¹⁷IPAC, California Institute of Technology, 1200 E. California Blvd, Pasadena, CA 91125, USA

¹⁸Caltech Optical Observatories, California Institute of Technology, Pasadena, CA 91125, USA

¹⁹INAF/IASF-Palermo, via Ugo La Malfa 153, I-90146, Palermo, Italy

²⁰Center for Gravitation, Cosmology and Astrophysics, Department of Physics, University of Wisconsin-Milwaukee, P.O. Box 413, Milwaukee, WI 53201, USA

²¹The eScience Institute, University of Washington, Seattle, WA 98195, USA

²²Ishigakijima Astronomical Observatory, National Astronomical Observatory of Japan, 1024-1 Arakawa, Ishigaki, Okinawa 907-0024, Japan

²³Department of Astronomy and Astrophysics, University of California, Santa Cruz, CA 95064, USA

²⁴Department of Physics and Astronomy, Rutgers, the State University of New Jersey, 136 Frelinghuysen Rd., Piscataway, NJ 08854, USA

²⁵Center for Computational Astrophysics, Flatiron Institute, 162 5th Avenue, New York, NY 10010, USA

²⁶Institute of Astronomy, National Tsing Hua University, Hsinchu 30013, Taiwan

²⁷Humboldt Universitaet zu Berlin, Newtonstrasse 15, 12489 Berlin, Germany

²⁸Institute of Physics, Humboldt-Universität zu Berlin, Newtonstr. 15, 124 89 Berlin, Germany

²⁹Deutsches Elektronensynchrotron, Platanenallee 6, D-15738, Zeuthen, Germany

³⁰Kavli Institute for Theoretical Physics, University of California, Santa Barbara, CA 93106, USA

³¹Research School of Astronomy and Astrophysics, Australian National University, Canberra, ACT 2611, Australia

³²Department of Astronomy, University of California, Berkeley, CA 94720-3411, USA

³³*Department of Particle Physics & Astrophysics, Weizmann Institute of Science, Rehovot 76100, Israel*

³⁴*Université Clermont Auvergne, CNRS/IN2P3, Laboratoire de Physique de Clermont, F-63000 Clermont-Ferrand, France*

³⁵*Jet Propulsion Laboratory, California Institute of Technology, Pasadena, CA 91109, USA*

³⁶*The Oskar Klein Centre & Department of Astronomy, Stockholm University, AlbaNova, SE-106 91 Stockholm, Sweden*

³⁷*Center for Interdisciplinary Exploration and Research in Astrophysics and Department of Physics and Astronomy, Northwestern University, 2145 Sheridan Road, Evanston, IL 60208, USA*

³⁸*Department of Physics, Tokyo Institute of Technology, 2-12-1, Ookayama, Meguro, Tokyo 152-8551, Japan*

ABSTRACT

The beginning of the third observing run by the network of gravitational-wave detectors has brought the discovery of many compact binary coalescences. Prompted by the detection of the first binary neutron star merger in this run (GW190425 / LIGO/Virgo S190425z), we performed a dedicated follow-up campaign with the Zwicky Transient Facility (ZTF) and Palomar Gattini-IR telescopes. As it was a single gravitational-wave detector discovery, the initial skymap spanned most of the sky observable from Palomar Observatory, the site of both instruments. Covering 8000 deg² of the inner 99% of the initial skymap over the next two nights, corresponding to an integrated probability of 46%, the ZTF system achieved a depth of ≈ 21 *m_{AB}* in *g*- and *r*-bands. Palomar Gattini-IR covered a total of 2200 square degrees in *J*-band to a depth of 15.5 mag, including 32% of the integrated probability based on the initial sky map. However, the revised skymap issued the following day reduced these numbers to 21% for the Zwicky Transient Facility and 19% for Palomar Gattini-IR. Out of the 338,646 ZTF transient “alerts” over the first two nights of observations, we narrowed this list to 15 candidate counterparts. Two candidates, ZTF19aarykkb and ZTF19aarzaod were particularly compelling given that their location, distance, and age were consistent with the gravitational-wave event, and their early optical lightcurves were photometrically consistent with that of kilonovae. These two candidates were spectroscopically classified as young core-collapse supernovae. The remaining candidates were photometrically or spectroscopically ruled-out as supernovae. Palomar Gattini-IR identified one fast evolving infrared transient after the merger, PG19bn, which was later spectroscopically classified as an M-dwarf flare. We demonstrate that even with single-detector gravitational-wave events localized to thousands of square degrees, systematic kilonova discovery is feasible.

1. INTRODUCTION

The third observing run (O3) by the network of gravitational-wave (GW) detectors with Advanced LIGO (Aasi et al 2015) and Advanced Virgo (Acerneese et al 2015) began in April 2019. This detector network has already observed over a score binary black holes thus far (Singer et al. 2019a; Shawhan et al. 2010; Chatterjee et al. 2019a; Singer et al. 2019b; Chatterjee et al. 2019b; Ghosh et al. 2019). The current discovery rate builds on the success of the first few observing runs, which yielded 10 binary black hole detections (Abbott et al. 2018).

In addition, the coincident discovery of the binary neutron star (BNS) merger GW170817 (Abbott et al. 2017a), a short gamma-ray burst (SGRB) GRB170817A (Abbott et al. 2017b; Goldstein et al. 2017; Savchenko et al. 2017), and its “kilonova” (KN) counterpart, AT2017gfo (Alexander et al. 2017; Chornock et al. 2017; Cowperthwaite et al. 2017; Drout et al. 2017; Evans et al. 2017; Haggard et al. 2017; Hal-

lin et al. 2017; Kasliwal et al. 2017; Kilpatrick et al. 2017; Margutti et al. 2017; McCully et al. 2017; Nicholl et al. 2017; Shappee et al. 2017; Pian et al. 2017; Smartt et al. 2017; Troja et al. 2017; Utsumi et al. 2017), initiated a new era of multi-messenger astronomy. Amongst many other science cases, measurements of the equation of state (EOS) of neutron stars (Bauswein et al. 2013; Abbott et al. 2017a; Radice et al. 2018; Bauswein et al. 2017; Coughlin et al. 2018), the formation of heavy elements (Just et al. 2015; Wu et al. 2016; Roberts et al. 2017; Abbott et al. 2017c; Rosswog et al. 2017; Kasliwal et al. 2019), and the expansion rate of the universe (Abbott et al. 2017; Hotokezaka et al. 2018) are all important results of the first BNS detection.

Following the success of GW170817, the Zwicky Transient Facility (ZTF) (Bellm et al. 2018; Graham et al. 2019; Dekany et al. 2019; Masci et al. 2018) on the Palomar 48 inch telescope, and Palomar Gattini-IR, a new wide-field near-infrared survey telescope at Palomar observatory, have been observing both SGRBs from the *Fermi* Gamma-ray Burst Monitor (Coughlin et al. 2018a; Cenko et al. 2018; Coughlin et al. 2018b,c,d; Ahumada et al. 2018; Coughlin et al. 2019a) and GW

* Moore-Sloan, WRF, and DIRAC Fellow

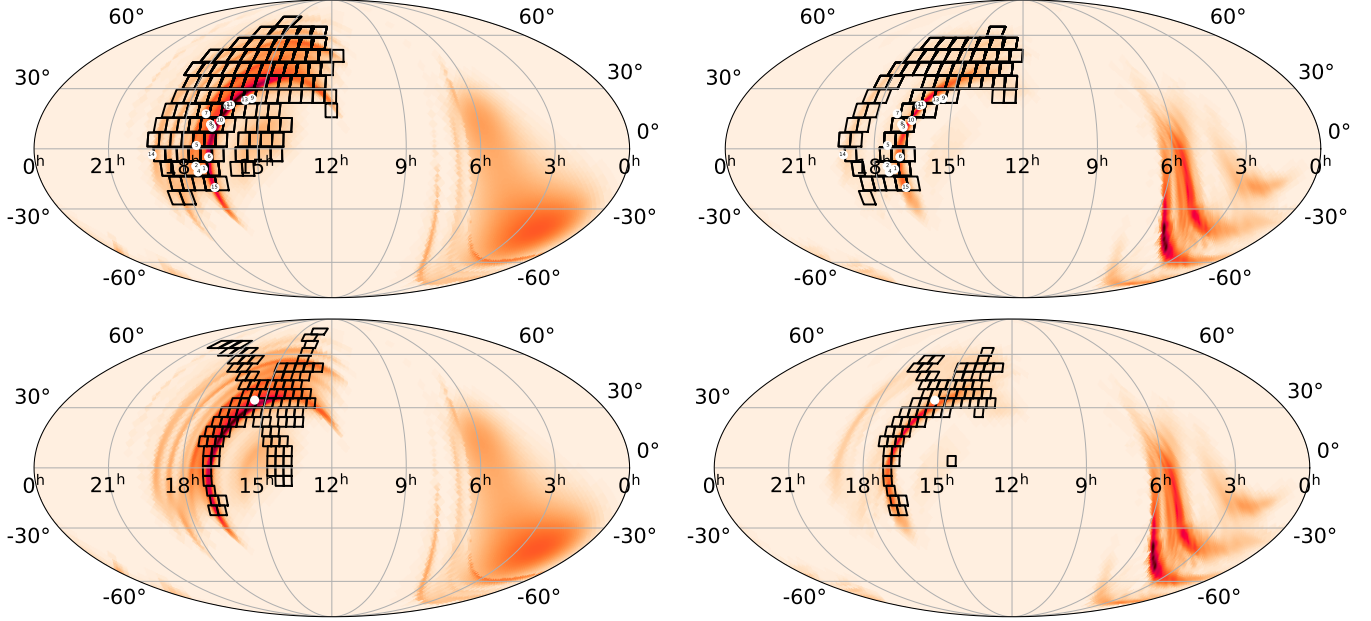


Figure 1. Coverage of GW190425. (Left) The top and bottom rows show the $\approx 47 \text{ deg}^2$ ZTF tiles and the $\approx 25 \text{ deg}^2$ Palomar Gattini-IR tiles respectively on the 90% probability region of the initial BAYESTAR skymap, along with the identified transients highlighted in Table 2. For the ZTF observations, the numbering scheme is 1: ZTF19aarykkb, 2: ZTF19aarzaod, 3: ZTF19aasckwd, 4: ZTF19aasfogy, 5: ZTF19aasejil, 6: ZTF19aaryxjf, 7: ZTF19aascxux, 8: ZTF19aasdajo, 9: ZTF19aasbamy, 10: ZTF19aasckq, 11: ZTF19aarycuy, 12: ZTF19aasbphu, 13: ZTF19aasbau, 14: ZTF19aarxxwb, 15: ZTF19aashlts. For Palomar Gattini-IR, we display the only identified transient, PGIR 19bn. (Right) We show the tilings of the two telescopes on the final LALInference map. We only include the tiles in the inner 90% probability region for each skymap.

events from LIGO. In addition to finding the “afterglow” associated with a highly relativistic jet powered by a SGRB (Wijers et al. 1997; Mészáros & Rees 1998; Ascenzi et al. 2019), our goal has been to identify a KN, the ultraviolet/optical/near-IR emission generated by the radioactive decay of r-process elements (Lattimer & Schramm 1974; Li & Paczynski 1998; Metzger et al. 2010; Roberts et al. 2011; Rosswog 2015; Kasen et al. 2017). The ZTF and Palomar Gattini-IR surveys are our discovery engines, and the Global Relay of Observatories Watching Transients Happen (GROWTH) network¹ is our follow-up network. GROWTH uses a variety of facilities worldwide across various wavelengths to perform rapid follow-up and classification of objects.

There are many survey systems participating in the searches for GW counterparts. Amongst many others, the Dark Energy Camera (DECam; Flaugher et al. 2015), the Gravitational-wave Optical Transient Observer (GOTO; O’Brien 2018), the Panoramic Survey Telescope and Rapid Response System (Pan-STARRS; Kaiser et al. 2010), the All-Sky Automated Survey for Supernovae (ASASSN; Shappee et al. 2014) and Asteroid Terrestrial-impact Last Alert System (ATLAS;

Tonry et al. 2018) all have performed observations of events during the third observing run. ZTF provides a competitive addition to these systems, given its depth ($m_{AB} \sim 20.6$ in 30 s), wide field of view (FOV $\approx 47 \text{ deg}^2$ per exposure), and average cadence of ~ 3 days over the entire accessible sky. In particular, the cadence is important for establishing candidate history when performing target of opportunity (ToO) observations. The SGRB program, that has covered localization regions spanning thousands of square degrees (Coughlin et al. 2019a), demonstrated that ZTF is capable of detecting GW170817-like sources out to the Advanced LIGO/Virgo detection horizon at about (~ 200 Mpc; Abbott et al. 2018). In addition, Palomar Gattini-IR (Moore & Kasliwal 2019, De et al. in prep.) is covering the entire visible northern sky every 2 nights to a J-band depth of $\approx 15.5 - 16$ AB mag. With its 25 deg^2 FOV and near-infrared sensitivity, Palomar Gattini-IR provides a complementary system for objects that are expected to be as red as KNe (Metzger 2017), albeit at lower sensitivity.

The first BNS detection of O3, GW190425 / LIGO/Virgo S190425z, was a single detector event discovered by the Advanced LIGO-Livingston detector, with Virgo also observing at the time (Singer et al. 2019b). Occurring at 2019-04-25 08:18:05 UTC, the estimated false

¹ <http://growth.caltech.edu/>

alarm rate was 1 in 70,000 years, with a high likelihood of being a binary neutron star. The first reported BAYESTAR skymap provided an extremely coarse localization, resulting from the low signal-to-noise ratio in Advanced Virgo; it spanned $\sim 10,000$ deg 2 , which is nearly a “pi of the sky.” The updated LALInference skymap (Singer et al. 2019c), released at 2019-04-26 15:32:37 UTC, reduced the localization region requiring coverage by $\approx 25\%$ to ~ 7500 deg 2 . The all-sky averaged distance to the source is 156 ± 41 Mpc.

This event serves to extend the frontier in searches for optical transients in large areas. The intermediate Palomar Transient Factory (iPTF) found optical counterparts to eight long GRBs localized to ~ 100 deg 2 (Singer et al. 2015), with GRB 130702A (Singer et al. 2013) being the first of its kind. During O1 and O2, iPTF and GROWTH followed-up several poorly localized binary black hole mergers (Kasliwal et al. 2016; Bhalerao et al. 2017). More recently, ZTF followed-up a SGRB discovered by the *Fermi* Gamma-Ray Burst Monitor, GRB180523, covering ~ 3000 deg 2 in the process (Coughlin et al. 2019a). In this paper, we describe an ~ 8000 square degree search for the KN counterpart to a single-detector GW event. Our campaign emphasizes the key role played by both large FOV telescopes like ZTF and Palomar Gattini-IR, as well as the associated follow-up systems. We demonstrate that our strategy for tiling the sky, vetting candidates, and pursuing follow-up is robust, and capable of promptly reducing 338,646 transient alerts from ZTF to a handful of interesting candidates for follow-up. Our paper is structured as follows. We describe our observing plan in Section 2. The identified candidates, including their follow-up, are detailed in Section 3. We summarize our conclusions and future outlook in Section 4.

2. OBSERVING PLAN

Because GW190425 came during Palomar night-time (2019-04-25 08:18:05 UTC), it occurred concurrently with ongoing survey observations by both ZTF and Palomar Gattini-IR. Within the 90% localization, approximately 44% of the original BAYESTAR map was observable from Palomar over the whole night, corresponding to ≈ 5000 deg 2 . The GW event was automatically ingested into the GROWTH ToO Marshal, a database we specifically designed to perform target-of-opportunity follow-up of events localized to large sky-error regions, including GW, neutrino, and gamma-ray burst events (Coughlin et al. 2019a). The ToO marshal displays the properties of each event, automatically fetches the associated skymap, facilitates observation planning, and allows us to directly trigger the

telescope queue for certain facilities to which GROWTH has access, namely ZTF, Palomar Gattini-IR, DECam, Kitt Peak EMCCD Demonstrator (KPED) on the Kitt Peak 84 inch telescope (Coughlin et al. 2019b), and the GROWTH-India telescope² (Bhalerao et al., in prep.).

Triggering ToO observations for survey instruments like ZTF and Palomar Gattini-IR halts their ongoing survey observations and redirects them to observe only certain fields as directed by an observation plan. The observation plan generated by the ToO marshal relies on `gwemopt` (Coughlin et al. 2018), a code that optimizes the telescope scheduling process for gravitational wave follow-up. `gwemopt` handles both synoptic and galaxy-targeted search strategies; we employed the former to conduct observations with some of our facilities, Palomar Gattini-IR, GROWTH-India and ZTF, and the latter for scheduling observations with KPED.

For synoptic searches, our scheduler code in `gwemopt` divides the skymap into a grid of “tiles” that are the shape and size of the FOV of the telescope based on the “ranked” tiling method (Ghosh et al. 2017). For ZTF, we generate tiles based on a predefined reference grid of already imaged fields. The code then determines the observable time segments for each tile throughout the night based on rising and setting of fields, and the need to make repeated exposures. We scheduled the observations described in this paper using the “greedy” algorithm, which selects the highest probability field available within each time window.

The coverage for both ZTF and Palomar Gattini-IR is shown in Figure 1. As dictated by the greedy scheduling algorithm, we managed to cover the highest probability region of the initial BAYESTAR skymap and final LAL-Inference skymap with both ZTF and Palomar Gattini-IR, though we were unable to tile the entire accessible localization due to its size.

2.1. ZTF

Serendipitously, after the neutron star merger time and before the GW alert was distributed, ZTF had already observed 1920 deg 2 of the sky in the *r*-band, corresponding to $\sim 12\%$ of the initial BAYESTAR map. This serendipitous overlap between ongoing survey observations and the LIGO-Livingston-only localization is unsurprising as both of the Advanced LIGO interferometers have maximum sensitivity in the sky overhead in North America (Finn & Chernoff 1993; Kasliwal & Nissanka 2014).

For each of the two nights of observation, we chose a synoptic observing strategy that was most appropri-

² <https://sites.google.com/view/growthindia/>

ate given the sky localization and time available for observation. On night 1, our observing strategy involved a sequence of *g-r-g* band exposure blocks; each exposure was 30 s, which is the normal duration of exposures during ZTF survey operation. The *g-r-g* sequence is the baseline observing strategy for GW follow-up with ZTF as it is specifically designed to capture the inter- and intra-night color evolution of GW170817-like KNe and to distinguish them from supernovae (Shappee et al. 2017; Kilpatrick et al. 2017). For these observations, we imposed the requirement that there should be reference images in *g* and *r* available for each field being scheduled.

We note that our observing strategy on the first night mostly amounted to a change in cadence of the observations to the survey, given the exposure time used and the sky localization covered. We chose to take 30 s exposures in order to cover the maximum possible probability with the 3 hours of time remaining for observation between triggering the telescope and the end of the night. On the first night, accounting for the loss in probability due to chip gaps and the processing success, ZTF covered 3250 deg², corresponding to about 36% of the initial BAYESTAR map.

On night 2 we modified our strategy, trading off the third *r*-band epoch for an increase in depth given the distance of 155 ± 45 and the expected photometric evolution. We increased the exposure time to 90 s, corresponding to an increase of ≈ 0.6 mags on the second night. Motivated by the increase in the accessible sky area, and the increase in available observation time (~ 5 more hours than the first night), we obtained one epoch in each of *g*- and *r*-band, corresponding to about 46% of the initial BAYESTAR map.

After our observations on both nights were complete, a new LALInference skymap was released (Ligo Scientific Collaboration & VIRGO Collaboration 2019). The LALInference runs reduced the skymap to ~ 7500 deg² and shifted more of the probability to two lobes near the sun and in the Southern hemisphere (see Figure 1). In summary, ZTF covered about 8000 deg² within the 99% integrated probability region. This corresponds to 46% of the probability in the original BAYESTAR skymap and 21% of the probability in the LALInference skymap. Our observations with ZTF over the two nights covered a 5 σ median depth of $m_{AB} = 21.0$ in *r*-band and $m_{AB} = 20.9$ in *g*-band.

2.2. Palomar Gattini-IR

Palomar Gattini-IR initiated target of opportunity observations of the localization region at 2019-04-25 09:12:09 UTC, which was 11 minutes after the initial no-

tice time. The synoptic tiling strategy was determined in the same way as for ZTF (Coughlin et al. 2018). Palomar Gattini-IR imaged a total of 2401 deg² of the localization region spread over 227 field tiles, covering 32% of the probability region of the BAYESTAR skymap and 19% for the LALInference localization. Each field visit consisted of a sequence of 8 dithered exposures of 8.1 s each, amounting to a total exposure time of 64.8 s per field. This resulted in a median stacked depth of $m_{AB} = 15.5$ in *J*-band. The real-time data reduction pipeline (De et al. in prep) reduced the data and identified transient candidates through the application of difference imaging using reference images of the fields.

2.3. GROWTH-India Telescope

The GROWTH-India telescope started observations at 2019-04-25 14:17:57 UTC, 6 hours after the trigger. The schedule calculated by the GROWTH ToO Marshal covered the peak of the northern localization region of the LALInference skymap. The 300 s exposures yielded a typical *r*-band limiting magnitude of $m_{AB} = 20.5$. The 33 overlapping images covered a total of 11.1 deg², corresponding to 0.54% enclosed probability.

2.4. Galaxy Targeted Follow-up

In addition to the synoptic surveys for counterparts, a subset of the available systems performed galaxy-targeted follow-up. The galaxy-targeted follow-up program relies on the Census of the Local Universe (CLU) catalog (Cook et al. 2017); it is complete to 85% in star-formation and 70% in stellar mass at 200 Mpc. The sky area coverage of galaxies is $\approx 1\%$ within these local volumes (Cook et al. 2017). This makes targeted galaxy pointing tractable for small FOV telescopes (see Arcavi et al. (2017) or Golkhou et al. (2018) for example). Of the galaxies within the volume, our work prioritizes them for follow-up as follows.

The GROWTH ToO Marshal uses an algorithm modified from LCO’s galaxy-targeted follow-up of GW events (Arcavi et al. 2017), which uses a combination of a galaxy’s location in the GW localization region (including the distance), S_{loc} , the galaxy’s absolute B-band luminosity, S_{lum} , and the likelihood of detecting a counterpart at the galaxy’s distance S_{det} . We define S_{det} as a prioritization of a transient’s potential brightness, taking a fiducial limiting magnitude, m_{lim} , for the exposures of $m_{AB} = 22$, and convert it to a limiting apparent luminosity L_{lim} . We also compute the luminosity for a potential transient with an absolute magnitude between -12 and -17 , using wide bounds to be robust against differences in intrinsic brightness. Then, S_{det} becomes $S_{\text{det}} = \frac{L_{\text{KNmax}} - L_{\text{KNmin}}}{L_{\text{KNmax}} - L_{\text{lim}}}$, that we limit to

be between 0.01 and 1. Our final metric is therefore $S = S_{\text{loc}} \times S_{\text{lum}} \times S_{\text{det}}$.

Beginning 4 hrs after the event, the Lulin One-meter Telescope (LOT) in Taiwan observed 85 galaxies in the initial 90% localization (Tan et al. 2019b,a). LOT used 180s exposures in R -band with seeing varying between 1.5-2.5 arcsec. Using comparisons to Pan-STARRS images, these exposures yielded a typical 5σ limiting magnitude of $m_{\text{AB}} = 20$. Similarly, KPED started the galaxy targeted follow-up 1.9 hours after the merger and continued until the first ZTF candidates came online. KPED imaged 10 galaxies in the r -band filter for 300 seconds, finding no visible transients up to $r = 20.8$ (Ahumada et al. 2019a). 300s is the fiducial time chosen for KPED to potentially reach limiting magnitudes of $m_{\text{AB}} = 22$, useful for both the transient discovery and follow-up (Coughlin et al. 2019b).

3. CANDIDATES

We now briefly describe the candidate filtering criteria for the ToO program for ZTF and Palomar Gattini-IR (see Coughlin et al. 2019a for further details). For GROWTH-India, LOT, and KPED, we did not identify any viable counterparts without previous history of variability in the analysis.

3.1. Candidates from ZTF

A ZTF transient alert is defined as a 5σ change in brightness in the image relative to the reference epoch. For ZTF, all transient alerts flagged for follow-up required at least two detections separated by 15 minutes in order to remove asteroids and other transient objects. We used the Pan-STARRS1 point source catalog (PS1 PSC; Tachibana & Miller 2018) to remove candidates associated with likely point sources (i.e., stars). Full details on the PS1 PSC can be found in Tachibana & Miller (2018); briefly, the authors build a machine learning model that determines the relative likelihood that a PS1 source is a point source or extended based on PS1 colors and shape measurements. The model is trained using sources observed with the *Hubble Space Telescope*, achieving an overall accuracy of $\sim 94\%$, and classifying $\sim 1.5 \times 10^9$ total sources.

We also used a real-bogus (RB) classifier to remove common image subtraction artifacts (Mahabal et al. 2019). This method consists of a random forest classifier trained with real objects and artifacts from ZTF images, separating objects with an accuracy of $\sim 89\%$. In order to capture the majority of real events, the threshold was set to $RB > 0.25$. In addition, the transients must have brightened relative to the reference image, leading to a positive residual after the image subtraction. Furthermore, the program excluded all objects within 20 arcsec

of $m_{\text{AB}} < 15$ stars to avoid artifacts from blooming. The final step involved constraining the search to events that have no historical detections prior to three days before the trigger.

This filtering scheme reduced the number of ZTF alerts from 50802 to 28 for the first night and from 287844 to 234 relevant candidates for the second night. A more detailed breakdown on the number of alerts that successfully met the criteria at each filtering step can be found in Table 1.

Table 1. Filtering results for both ZTF nights. The quantities represent the number of alerts that passed a particular step in the filter. Each step is run over the remaining alerts from the previous stage. The criteria are described in Section 3.1 and the total number of relevant candidates is highlighted.

Filtering criteria	# of Alerts on April-25	# of Alerts on April-26
ToO alerts	50,802	287,844
Positive subtraction	33,139	182,095
Real	19,990	118,446
Not stellar	10,546	61,583
Far from a bright source	10,045	58,881
Not moving	990	5,815
No previous history	28	234

The candidates that passed these criteria were filtered and displayed by the GROWTH Marshal, a tool developed for astronomers to have unified access to discovery streams and to coordinate follow-up observations (Kasliwal et al. 2019a). The GROWTH Marshal contains historical lightcurves (including upper limits) for each object and also performs cross-matches with external catalogs.

We subjected each of the remaining candidates to a thorough human vetting process to determine whether the transient could be a viable counterpart to GW190425. Through this vetting process, we removed candidates whose coordinates were outside the 90% contour in the GW localization, and candidates that had archival detections in the Pan-STARRS1 Data Release 2 (Flewelling 2018). We flagged Active Galactic Nuclei (AGN) based on the WISE colors (Wright et al. 2010) for each transient and its offset from the nucleus of the galaxy. Furthermore, we prioritized candidates whose photometric/spectroscopic redshift was consistent with the GW distance estimate, and whose extinction-corrected lightcurve exhibited rapid color evolution initially. For the most promising candidates in our vetted list, we performed forced photometry at

the position of the source to ensure there were no historical detections with ZTF.

Our first night of observations yielded only two such candidates that passed both the automatic filtering and human vetting processes. These two candidates ZTF19aarykkb and ZTF19aarzaod. During the second night, we identified 13 additional transients through filtering and human vetting. The second night of observations allowed us to obtain an additional candidates detected on the first night that were consistent with the new skymap, thereby increasing our candidate list from the first night to the second. We describe the most promising of these 15 candidates in more detail in Sec. 3.3.

To double-check that we did not miss any candidates, we used *Kowalski*³, an open-source system used internally at Caltech (primarily) to archive and access ZTF’s alerts and light curves (Duev et al., in prep.). Specifically, we used *Kowalski*’s web-based GUI called the ZTF Alert Lab (ZAL), with which users can efficiently query, search and preview alerts. Our results were consistent with the results above. To triple-check that we did not miss any candidates, we also carried out an additional automatic search of the AMPEL alert archive (Nordin et al. 2019) for transients that might have escaped. No additional candidates from either night were found.

3.2. Candidates from Palomar Gattini-IR

For Palomar Gattini-IR, we adopted the following selection criteria for human vetting of sources identified in the difference imaging:

1. We selected candidates that were at least 1 arcminute away from bright stars with $m_J < 10$, excluding $\sim 0.7\text{--}2\%$ of the imaged region, in order to remove contamination from subtraction artifacts.
2. The first detection of the candidate must have been after the gravitational-wave trigger time.
3. An object must have at least two detections with a signal-to-noise ratio greater than 5 or a signal-to-noise ratio greater than 7 in one detection. Amongst sources with single detections, we also rejected known asteroids.

The only viable candidate identified from sources with multiple detections was PGIR 19bn, a fast rising transient within the localization region that was detected 3 times in images taken *after* the merger. The previous

upper limit at the location was from 2 days before the merger (Figure 2). The location of PGIR 19bn is consistent with a faint ($r \approx 23$ mag) source in SDSS, that was photometrically classified as a galaxy with a photo-z of 0.59. In order to confirm the classification of the source, we obtained a spectrum of the SDSS counterpart with LRIS on the Keck-I telescope on 2019-06-03, as shown in Figure 2. The spectrum shows broad absorption bands of TiO and VO, consistent with a galactic M-dwarf, suggesting that PGIR 19bn was a M-dwarf flare.

3.3. Follow-up of ZTF candidates

The 15 sources that were identified from ZTF observations are shown in Table 2 and on Figure 1. Using a variety of resources including the SED Machine (SEDM) (Blagorodnova et al. 2018; Rigault et al. 2019) on the Palomar 60 inch (P60) telescope, the Double Beam Spectrograph (DBSP; Oke & Gunn 1982) on the Palomar 200 inch (P200) telescope, the Robert Stobie Spectrograph (RSS; Smith et al. 2006) on the Southern African Large Telescope (SALT), the Liverpool telescope (LT; Steele et al. 2004), the GROWTH-India telescope, the KPED, the Discovery Channel Telescope (DCT) and LOT, we followed up each of these candidates with further photometry and/or spectroscopy.

We classified 5 objects using spectroscopy and tracked the color evolution of 15 objects using photometry. A KN is expected to show a rapid evolution in magnitude (Metzger 2017); GW170817 faded $\Delta r \sim 1$ mag per day over the first 3 days and by $\Delta r \sim 4.2$ mags total around day 10. Thus, we can use photometric lightcurves to determine whether a transient is consistent with the expected evolution for a KN. Some photometrically monitored transients showed evolution that was too slow ($\Delta r \sim 0.1$ mag per day) to be consistent with GW170817 or kilonova model predictions. Many other candidates highlighted in Kasliwal et al. 2019b were observed with GROWTH facilities, however, they were later excluded by the updated LALInference skymap. In addition to these sources, we reported objects in Kasliwal et al. 2019b with ZTF detections before the event time to the community in order to limit the number of false positives identified by other surveys that may not have recently imaged those areas of the sky.

We now provide a broad summary of the most promising candidates ruled out by spectroscopy, as examples of the follow-up performed by the GROWTH facilities when vetting candidates. In particular, we highlight the lightcurves of ZTF19aarykkb, ZTF19aarzaod, ZTF19aasckkq, and ZTF19aasckwd in the top left, top right, lower left and lower right panels respectively in Figure 3 and discuss them briefly below. The associated

³ <https://github.com/dmitryduev/kowalski>

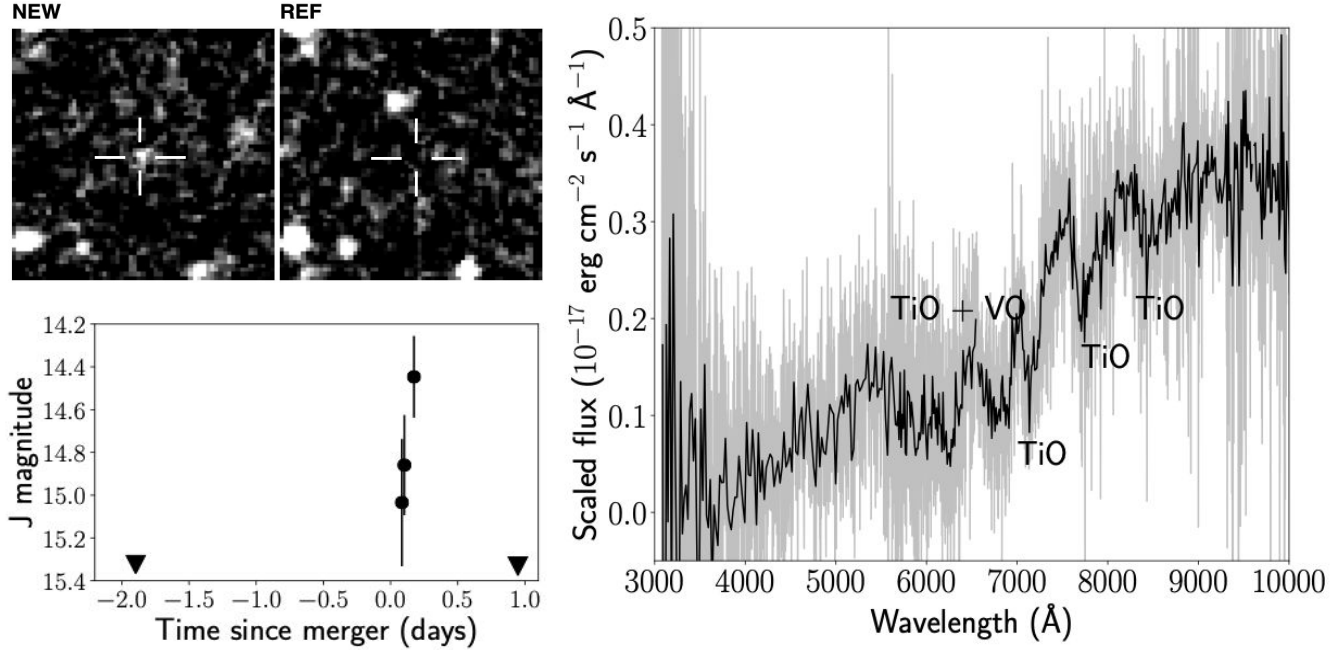


Figure 2. Discovery image, photometry and spectroscopic follow-up of PGIR 19bn. (Left) Top panels show the discovery and reference image of PGIR 19bn in J-band, found in follow-up observations of S190425z. We note that the reference image is deeper than the science image by ~ 1.5 mag, so fainter objects will appear prominent in the reference image even when they are not detected in the science image. The lower panel shows a light curve of the transient from forced photometry on the images (circles are detections while inverted triangles are upper limits). (Right) Optical spectrum of the SDSS counterpart of PGIR 19bn obtained with Keck LRIS (grey lines are raw spectra, while the black lines are binned), showing absorption bands of TiO and VO consistent with a galactic M-dwarf.

spectra are shown in the top panel of Figure 4; the spectrum of ZTF19aasckwd is not shown as we only have a spectrum of the galaxy host. ,

3.3.1. ZTF19aarykkb

We first detected the transient ZTF19aarykkb 2.13 hours after the merger and highlighted it in the first ZTF GCN (Kasliwal et al. 2019b). ZTF19aarykkb is 12.1 arcsec offset from the host galaxy, which is at a redshift of $z = 0.024$, corresponding to a luminosity distance of 106 Mpc. The absolute magnitude of the discovery is $g = -15.9$, broadly consistent with GW170817 and KNe predictions. Archival data showed no variability in the region before the merger. Due to its distance and discovery mag, several facilities followed-up this source (Perley et al. 2019a; Burke et al. 2019; Morihana et al. 2019a; Dichiara et al. 2019; Rhodes et al. 2019; Nicholl et al. 2019; Chang et al. 2019b) The LOT group in Taiwan imaged the object 6 hours after the transient set in Palomar (Tan et al. 2019b); later that day, the LT continued the monitoring. On average, this object was imaged every 1.3 hours within the first 26 hours after the merger. The first spectrum for this object came from the Himalayan Chandra Telescope (HCT) about 10.67 hours after the trigger (Pavava et al. 2019), show-

ing a strong $\text{H}\alpha$ line at a redshift of $z = 0.024$. This was confirmed 8 hours later by the LT team with the Spectrograph for the Rapid Acquisition of Transients (SPRAT) (Piascik et al. 2014), who classified it as a young SN Type II (Perley et al. 2019a), based on the characteristic P-Cygni profile in the LT spectrum. An additional spectrum was taken about 10 hours later with the DeVeley spectrograph mounted on the 4.3 m DCT (Dichiara et al. 2019), showing similar strong $\text{H}\alpha$, furthermore confirming the SN classification (see Figure 4).

3.3.2. ZTF19aarzaod

ZTF19aarzaod was first detected by ZTF 2.15 hrs after the merger (Kasliwal et al. 2019b) with no previous history of variability up to $g > 20.01$. The redshift of the host galaxy is $z = 0.028$, putting the transient at a distance of 128.7 Mpc. The transient is offset by 8.2 arcsec from the host galaxy and its absolute magnitude at discovery was $r = -15.3$, also consistent with a GW170817-like KN. ZTF19aarzaod was extensively followed-up with various observatories (Hiramatsu et al. 2019; Buckley et al. 2019; Izzo et al. 2019; Wiersema et al. 2019; Castro-Tirado et al. 2019; Morihana et al. 2019a; Rhodes et al. 2019; Nicholl et al. 2019) and on average was imaged every 1.7 hours during the first day.

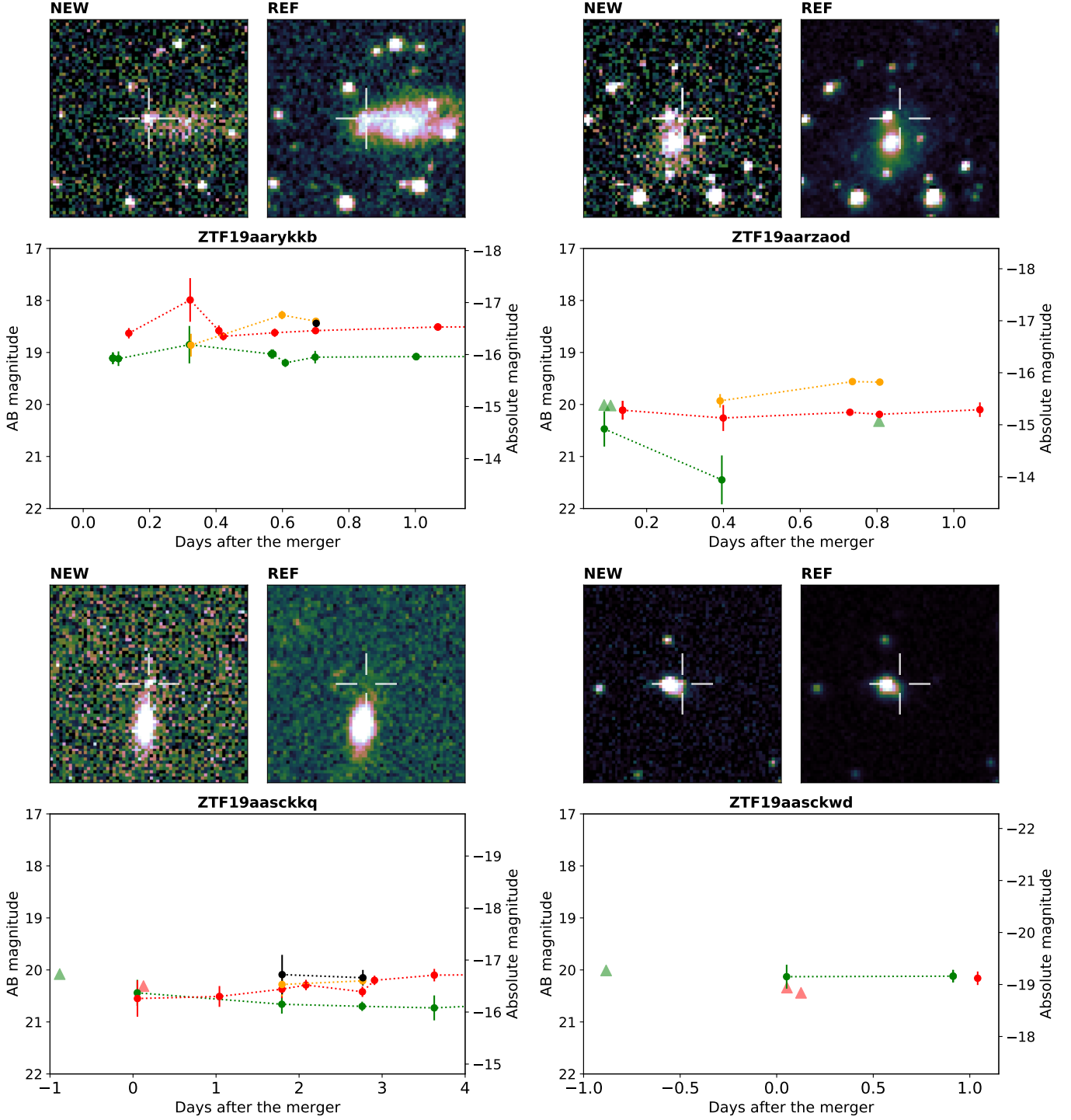


Figure 3. Lightcurves and r-band cutouts for the ZTF candidates discussed in Section 3.3. The lightcurves are constructed with data acquired with GROWTH facilities: for ZTF19aarykkb, the data is from ZTF, LOT, GIT and LT, for ZTF19aarzaod, ZTF, LOT and LT, for ZTF19aasckkq, ZTF, KPED and LT and for ZTF19aasckwd, ZTF and KPED. We used colors to represent each band in the lightcurves: green for g-band, red for r-band, yellow for i-band and black for z-band. While triangles in the lightcurve represent upper limits, filled circles are the magnitudes of the object. For each transient, the cutout on the left corresponds to the ZTF discovery image and the right cutout corresponds to the ZTF reference image of the host. A cross marks the location of the transient in the reference image. The cutouts are 0.7 sq. arcmin with north being up and east to the left.

Spectroscopic observations of ZTF19aarzaod were taken

with RSS mounted on SALT on UT 2019-04-26.0 under

a special gravitational-wave follow-up program 2018-2-GWE-002 and reduced with a custom pipeline based on PyRAF routines and the PySALT package (Crawford et al. 2010). The spectrum covered a wavelength range of 470-760 nm with a spectral resolution of $R = 400$. The spectrum shows broad $\text{H}\alpha$ emission along with some He I features (see Fig. 4) classifying it as a type II supernova at $z = 0.028$ (Buckley et al. 2019).

3.3.3. *ZTF19aasckkq*

The transient ZTF19aasckkq (Anand et al. 2019) was first detected by ZTF 1.23 hrs after the merger. It is offset from the host galaxy by 10.1 arcsec, and its last upper limit ($m_{\text{AB}} > 20.1$ in g -band) was the night before the merger. The discovery absolute mag is $r = -16.3$, similar to GW170817 at peak. ZTF19aasckkq was followed-up 18 hours after the last ZTF detection by LT and KPED (Ahumada et al. 2019b). On average, this transient was monitored every 5.8 hrs for a period of 3.8 days by a variety of observing groups (Perley et al. 2019b,c; Ahumada et al. 2019b,c). Nicholl et al. 2019 first posited that ZTF19aasckkq was a Type IIb SN at $z \sim 0.05$, consistent with the galaxy redshift (Hosseinzadeh et al. 2019). In Figure 4, we highlight the presence of He I, $\text{H}\alpha$ and $\text{H}\beta$ absorption features in the first spectrum we acquired with P200+DBSP, confirming its classification as a SN IIb at a redshift of $z = 0.0528$. The source was still bright at $r = 19.8$, 14 days after GW190425.

3.3.4. *ZTF19aasckwd*

ZTF19aasckwd was detected 1.23 hrs after the merger about 4.2 arcsec from its host galaxy (Anand et al. 2019). Its last upper limit ($m_{\text{AB}} > 20.1$ in g -band) was the night before the trigger. This transient was imaged every 8.1 hrs during the first day and it was classified as a SN Ia by Nicholl et al. (2019) at a redshift of $z = 0.145$ (Hosseinzadeh et al. 2019). The absolute magnitude at discovery was $r = -19.2$, a few magnitudes brighter than what is expected from a KN.

3.4. *Follow-up of non-ZTF candidates*

Here, we report on the follow-up triggered by the GROWTH team of a number of transients discovered by other facilities to be consistent with the LALInference skymap. We queried the GROWTH follow-up marshal at the positions of the most promising transients announced in order to determine whether 1) the transient had historical detections with ZTF, or 2) our concurrent photometry of the object also supported the KN hypothesis. Additionally, we used LT, GROWTH-India Telescope, and DECam to obtain photometry of the candidates that were not detected with ZTF because they were either fainter than the ZTF average upper limits or

inaccessible due to their sky location. Table 3 summarizes the most relevant non-GROWTH objects followed-up by the GROWTH collaboration, and we briefly discuss them below.

3.4.1. *Swift’s Ultraviolet/Optical Telescope (UVOT) candidate*

We followed up photometrically the *Swift*/UVOT candidate (Breeveld et al. 2019), discovered at RA=17:02:19.2, Dec=−12:29:08.2 in u -band with $m_{\text{Vega}} = 17.7 \pm 0.2$. The transient was within a few hundred arcseconds of two galaxies within the localization volume. After its initial detection with Swift, several other facilities (Breeveld et al. 2019; Kong et al. 2019; Andreoni et al. 2019b; Waratkar et al. 2019; De et al. 2019; Arcavi et al. 2019; Shappee et al. 2019; Im et al. 2019; Hu et al. 2019; Chang et al. 2019a; Tanvir et al. 2019; Troja et al. 2019; Morihana et al. 2019b; Kann et al. 2019), including ZTF and Palomar Gattini-IR, reported non-detections or pre-discovery upper limits that indicated the transient might be rapidly fading in the ultraviolet. Palmese et al. 2019 reported an object offset by < 1 arcsec from the position of the reported UVOT candidate after visually inspecting archival DECam optical images. Using the GROWTH-DECam program, Bloom et al. 2019 detected a source consistent with the coordinates reported by Palmese et al. 2019, but no transient at the coordinates reported by Swift (Kong et al. 2019) (see Table 3). The slight trailing observed in images of the original UVOT source (which introduced uncertainty in the astrometry) strongly hinted at the physical association between the transient and the offset source. The colors of the associated source ($r - z = 1.53$ and $g - r > 0.97$) are consistent with those of a M2-dwarf (West et al. 2011). For this reason, a likely explanation for the observed ultraviolet transient is that it was a galactic M2-dwarf flare (Lipunov et al. 2019a; Bloom et al. 2019), unassociated with the GW event.

3.4.2. *AT2019ebq/PS19qp*

We also obtained spectroscopy of AT2019ebq/PS19qp (Smith et al. 2019) with the Near-Infrared Echelle Spectrometer (NIRES) on Keck II. This candidate was initially claimed to be exceptional in that its optical spectrum taken with the Gran Telescopio Canarias (GTC) contained broad absorption features “unlike normal supernovae;” therefore Jonker et al. (2019) highlighted it as a promising KN candidate. Our NIR spectrum taken ~ 1.5 days after the trigger, however, exhibited broad P Cygni SN-like features of He I that indicated that the transient was a Type Ib/c SN (Jencson et al. 2019), ruling out its association with GW190425 (see bottom panel of Fig. 4). Several other facilities that

also followed up this source helped verify its classification (Schady et al. 2019; Morokuma et al. 2019; Jencson et al. 2019; McCully et al. 2019; Lipunov et al. 2019b; Carini et al. 2019; Dimitriadis et al. 2019).

7 additional PS1 candidates were ruled out based on previous ZTF detections (Andreoni et al. 2019a; see Table 3).

3.4.3. Marginal ATLAS candidates

Additionally, we acquired a short sequence (40 seconds each in *gri* filters) of imaging at the locations of all five of the marginal ATLAS transients reported by McBrien et al. (2019) using IO:O on the 2 m Liverpool Telescope (Perley & Copperwheat 2019). No significant source was detected at the location of any of them (to typical depths of 22 mag; see Table 3). Combined with the fact that none of these transients had a detectable host galaxy, this suggests these transients were likely to be spurious or perhaps short-timescale flares from faint stars.

4. CONCLUSIONS

In this paper, we have described the first follow-up of a binary neutron star event with ZTF and Palomar Gattini-IR. Covering more than 8000 deg^2 with ZTF and 2400 deg^2 with Palomar Gattini-IR over the next two nights, we show how these systems in combination with follow-up facilities are capable of rapidly identifying and characterizing transients on hour to day timescales over sky regions of this size. We show how it is possible to reduce 338,646 alerts to 15 previously unidentified candidate counterparts. We also show how with the follow-up resources available to GROWTH, we can rule out these objects as viable candidates.

Assuming an optical/NIR counterpart with a luminosity similar to that of GW170817, which had an absolute magnitude of about -16 in *g*, *r*, and *J*-bands, the apparent magnitude in these bands for the distribution of distances to GW190425 is $m_{AB} \approx 19 - 20.5$. This varies between 1 mag brighter than to near the detection limit for ZTF for this analysis, indicating ZTF is well-primed for detecting a GW170817-like source at these distances. We expect that a closer or brighter than expected source should be detectable with Palomar Gattini-IR.

As a cross-check of the number of sources we are identifying, we compare to the fiducial supernova rate of $\approx 10^{-4} \text{Mpc}^{-3} \text{yr}^{-1}$ (Li et al. 2011). The 90% localization volume of the gravitational-wave skymap is $\sim 2.1 \times 10^7 \text{Mpc}^3$. As stated above, ZTF covered about 46% of the skymap, meaning we expect to detect $\sim 2.1 \times 10^7 \text{Mpc}^3 \times 1.04 \times 10^{-4} \text{Mpc}^{-3} \text{yr}^{-1} \times 0.46 \approx 2.7 \text{day}^{-1}$. Since the distribution of Type II SNe at peak luminosity falls between absolute magnitudes of ≈ -15 to -20 mags

(Richardson et al. 2014), brighter than the expected distribution at peak for KNe, our follow-up observations with ZTF should have detected all of the bright, and most of the dim Type II SNe. Having taken images for about 12 hrs during the nights, we would expect to detect $\sim 1-2$, consistent with the 2 young supernovae highlighted in this paper.

Going forward, prioritizing further automatized classification of objects can lead to more rapid follow-up and dissemination of the most interesting objects. For example, the inclusion of machine-learning based photometric classification codes such as RAPID (Muthukrishna et al. 2019) will help facilitate candidate selection and prioritization. We are also actively improving the scheduling optimization, including examining the use of the “secondary” ZTF grid, that is designed to fill in the chip gaps.

The follow-up of GW190425 highlights two important points. The first is that rapid dissemination of updated GW skymaps is useful for tiling prioritization. This helps mitigate the effects of shifting localization regions, including potentially decreasing sky areas. The second is that we are capable of performing nearly all-sky searches with ZTF and Palomar Gattini-IR and conducting the necessary follow-up with partner facilities, even in the case of a single-detector GW trigger. One caveat to this conclusion is that in general, single-detector localizations will include regions on the sky not accessible to one ground-based facility alone; this motivates the use of coordinated networks of telescopes with worldwide coverage (Nissanke et al. 2013; Kasliwal & Nissanke 2014). But we have demonstrated that the network on hand is capable of overcoming the challenges of rapidly and efficiently searching for electromagnetic counterparts in this new era of gravitational-wave astronomy.

We would like to thank Peter Nugent for comments on an early version of this paper.

This work was supported by the GROWTH (Global Relay of Observatories Watching Transients Happen) project funded by the National Science Foundation under PIRE Grant No 1545949. GROWTH is a collaborative project among California Institute of Technology (USA), University of Maryland College Park (USA), University of Wisconsin Milwaukee (USA), Texas Tech University (USA), San Diego State University (USA), University of Washington (USA), Los Alamos National Laboratory (USA), Tokyo Institute of Technology (Japan), National Central University (Taiwan), Indian Institute of Astrophysics (India), Indian Institute of Technology Bombay (India), Weizmann Institute of Science (Israel), The Oskar Klein Centre at

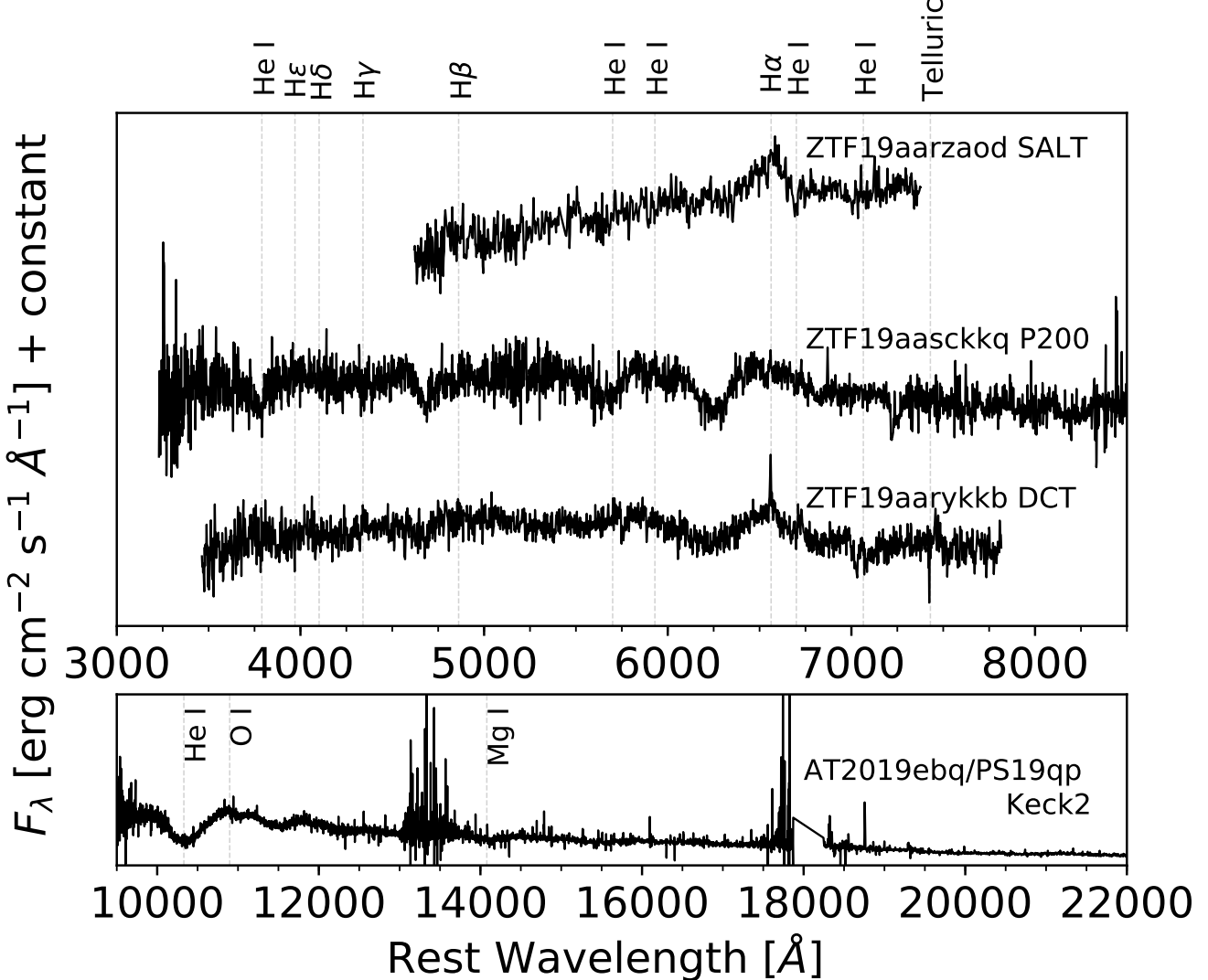


Figure 4. Spectra of all the candidates for which spectroscopic data were taken. The transient name and instrument used to obtain the spectrum are noted on the right hand side of the plot. We show the spectrum for AT2019ebq/PS19qp in its own panel given the different wavelengths covered from the other transients. The dotted gray lines show the characteristic features in each spectrum that helped with its classification. These four transients were all classified as core-collapse SNe. The classification and phase for each transient is as follows: ZTF19aasckkq - SN IIb, 7 days; ZTF19aarykkb - SN II, 1 day (Dichiara et al. 2019); ZTF19aarzaod - SN II, 0 days (Buckley et al. 2019); AT2019ebq/PS19qp - SN Ib/c, 1 day (Jencson et al. 2019).

Stockholm University (Sweden), Humboldt University (Germany), Liverpool John Moores University (UK) and University of Sydney (Australia).

Based on observations made with the Liverpool Telescope operated on the island of La Palma by Liverpool John Moores University in the Spanish Observatorio del Roque de los Muchachos of the Instituto de Astrofisica de Canarias with financial support from the UK Science and Technology Facilities Council. Based on observations obtained with the Samuel Oschin Telescope 48-inch and the 60-inch Telescope at the Palomar Observatory as part of the Zwicky Transient Facil-

ity project. ZTF is supported by the National Science Foundation under Grant No. AST-1440341 and a collaboration including Caltech, IPAC, the Weizmann Institute for Science, the Oskar Klein Center at Stockholm University, the University of Maryland, the University of Washington, Deutsches Elektronen-Synchrotron and Humboldt University, Los Alamos National Laboratories, the TANGO Consortium of Taiwan, the University of Wisconsin at Milwaukee, and Lawrence Berkeley National Laboratories. Operations are conducted by COO, IPAC, and UW. This research used resources of the National Energy Research Scientific Comput-

Table 2. Follow-up table for the Palomar Gattini-IR candidate described in Section 3.2 and the 15 most interesting ZTF candidates from Kasliwal et al. (2019b) and Anand et al. (2019). The sources with a star (*) have photometric evolution inconsistent with the evolution of a KN (Section 3.3). Spectra obtained with SALT (Buckley et al. 2019) and SOAR (Nicholl et al. 2019) were critical in classifying ZTF19aarzaod, ZTF19aasckwd, and ZTF19aasckkq. GROWTH teams acquired spectra of ZTF19aarykkb with HCT, LT, and DCT (Pavana et al. 2019; Perley et al. 2019a; Dichiara et al. 2019) and also provided useful photometric data towards the classification of these transients (Perley et al. 2019b; Ahumada et al. 2019b; Bhalerao et al. 2019; Ahumada et al. 2019a; Tan et al. 2019b).

Candidate	Coordinates (RA, Dec)	Discovery Mag.	Classification	Spectroscopic facilities	Phot. evolution [mag/day]
PG19bn	15:29:37.43 +33:57:37.0	J = 15.0	M-Dwarf	KECK LRIS	...
ZTF19aarykkb	17:13:21.95 -09:57:52.1	r = 18.63	SNII z=0.024	HCT, LT, DCT	...
ZTF19aarzaod	17:31:09.96 -08:27:02.6	r = 20.11	SNIIn z=0.028	SALT	...
ZTF19aasckwd	16:52:39.45 +10:36:08.3	r = 20.15	SN Ia z=0.145	SOAR	...
ZTF19aasckkq	16:33:39.14 +13:54:36.7	g = 20.86	SN IIb z=0.052	P200, SOAR	...
ZTF19aasbphu	16:22:19.95 +21:24:29.5	r = 19.71	Nuclear*	...	0.11
ZTF19aaryxjf	16:58:22.87 -03:59:05.1	g = 19.95	SN*	...	-0.014
ZTF19aarxxwb	19:14:46.40 -03:00:27.0	g = 18.89	SN*	...	0.12
ZTF19aasdajo	16:57:25.21 +11:59:46.0	g = 20.7	SN*	...	0.045
ZTF19aasbamy	15:25:03.76 +24:55:39.3	g = 20.66	SN*	...	0.01
ZTF19aarycuy	16:16:19.97 +21:44:27.4	r = 20.07	SN*	...	0.02
ZTF19aasbau1	15:40:59.91 +24:04:53.8	g = 20.49	SN*	...	0.01
ZTF19aasejil	17:27:46.99 +01:39:13.4	g = 20.53	SN*	...	0.01
ZTF19aascxux	17:13:10.39 +17:17:37.9	g = 20.56	SN*	...	0.06
ZTF19aashlts	16:52:45.01 -19:05:38.9	r = 19.95	SN*	...	0.03
ZTF19aasfogv	17:27:22.32 -11:20:01.9	g = 20.53	SN*	...	0.01

ing Center, a DOE Office of Science User Facility supported by the Office of Science of the U.S. Department of Energy under Contract No. DE-AC02-05CH11231. The 0.7m GROWTH-India Telescope (GIT) is set up by the Indian Institute of Astrophysics (IIA) and the Indian Institute of Technology Bombay (IITB) with support from the Indo-US Science and Technology Forum (IUSSTF) and the Science and Engineering Research Board (SERB) of the Department of Science and Technology (DST), Government of India Grant No. IUSSTF/PIRE Program/GROWTH/2015-16. It is located at the Indian Astronomical Observatory, IIA at Hanle, Ladakh (India). This publication has made use of data collected at Lulin Observatory, partly supported by MoST grant 105-2112-M-008-024-MY3. The KPED team thanks the National Science Foundation and the National Optical Astronomical Observatory for making the Kitt Peak 2.1-m telescope available. We thank the observatory staff at Kitt Peak for their efforts to assist Robo-AO KP operations. The KPED team thanks the National Science Foundation, the National Optical Astronomical Observatory, the Caltech Space Innovation Council and the Murty family for support in the building and operation of KPED. SED Machine is based upon work supported by the National Science Foundation under Grant No. 1106171. The Palomar Gattini-IR project thanks the Mount Cuba Foundation, Heising

Simons Foundation, the ANU Futures Scheme, the Bi-national Science Foundation and Caltech for generous support.

G.C. Anupama and Varun Bhalerao acknowledge partial support from SERB and IUSSTF. J. Sollerman acknowledges support from the Knut and Alice Wallenberg Foundation. E. Ofek is grateful for support by a grant from the Israeli Ministry of Science, ISF, Minerva, BSF, BSF transformative program, and the I-CORE Program of the Planning and Budgeting Committee and The Israel Science Foundation (grant No 1829/12). P. Gatkine is supported by NASA Earth and Space Science Fellowship (ASTRO18F-0085). C.-C. Ngeow, A. Patil and P.-C. Yu thank the funding from Ministry of Science and Technology (Taiwan) under grants 104-2923-M-008-004-MY5, 106-2112-M-008-007, 107-2119-M-008-012, 107-2119-M-008-014-MY2. E. Bellm and V. Z. Golkhou acknowledge support from the University of Washington College of Arts and Sciences, Department of Astronomy, and the DIRAC Institute. University of Washington’s DIRAC Institute is supported through generous gifts from the Charles and Lisa Simonyi Fund for Arts and Sciences, and the Washington Research Foundation. E. Bellm acknowledges support from the Large Synoptic Survey Telescope, which is supported in part by the National Science Foundation through Cooperative Agreement 1258333 managed by the Association of

Table 3. GROWTH follow-up table for candidates reported by other surveys. GROWTH-India, LOT, and DECam-GROWTH follow-up of the Swift/UVOT candidate discovered by Breeveld et al. (2019) helped confirm its classification as a likely M-dwarf flare (Breeveld et al. 2019; Kong et al. 2019; Andreoni et al. 2019b; Waratkar et al. 2019; De et al. 2019; Arcavi et al. 2019; Palmese et al. 2019; Shappee et al. 2019; Im et al. 2019; Hu et al. 2019; Chang et al. 2019a; Lipunov et al. 2019a; Tanvir et al. 2019; Troja et al. 2019; Bloom et al. 2019; Morihana et al. 2019b; Kann et al. 2019). Our initial Keck spectrum of another promising candidate, AT2019ebq/PS19qp (Smith et al. 2019) showed it was a Type II SN (Jencson et al. 2019). Several of the PS1 candidates reported by Smith et al. (2019), as well as Gaia19bpt (Kostrzewska-Rutkowska et al. 2019) were found to have previous detections with ZTF (Andreoni & Bellm 2019; Coughlin et al. 2019). For these sources, we list the number of days before GW190425 that they were detected in parentheses. LT provided constraining upper limits of some reported ATLAS candidates (McBrien et al. 2019; Perley & Copperwheat 2019).

Candidate	Coordinates (RA, Dec)	Discovery Mag.	GROWTH follow-up	upper limits
UVOT	17:02:19.21 –12:29:08.2	u=17.74	GIT, LOT, DECAM	DECam g > 24.0
...	DECam r > 24.0
...	DECam i > 23.7
...	DECam z > 23.1
AT2019ebq-PS19qp	17:01:18.33 –07:00:10.4	i= 20.40	Keck spectrum SN Ib/c	...
Gaia19bpt	14:09:41.88 +55:29:28.1	o = 18.49	ZTF19aarioci (4.12)	...
AT2019ebu-PS19pp	14:19:49.43 +33:00:21.7	i = 20.77	ZTF19aasbgll (2.10)	...
AT2019ebw-PS19pq	15:02:17.02 +31:14:51.6	i = 20.92	ZTF19aasazok (11.95)	...
AT2019ecc-PS19pw	15:26:29.53 +31:39:47.5	i = 20.10	ZTF19aapwgpg (17.96)	...
AT2019eck-PS19qe	15:44:24.53 +32:41:11.0	i = 20.81	ZTF19aapfrrw (24.97)	...
AT2019ecl-PS19qg	15:48:11.85 +29:12:07.1	i = 20.51	ZTF19aasgwnp (25.89)	...
AT2019ebr-PS19qj	16:35:26.48 +22:21:36.4	i = 19.79	ZTF18aaoxrvr (25.86)	...
AT2019ebo-PS19qn	16:54:54.71 +04:51:31.5	i = 20.02	ZTF19aarpbau (9.87)	...
AT2019eao-ATLAS19hyo	13:01:18.63 +52:09:02.1	o = 19.36	LT	g > 22.1
AT2019ebn-ATLAS19hwh	13:54:47.42 +44:46:27.3	o = 19.07	LT	g > 22.1
AT2019ebm-ATLAS19hwn	12:59:58.58 +29:14:30.7	o = 19.42	LT	g > 22.3
AT2019ebi-ATLAS19hyx	14:32:31.53 +55:45:00.1	o = 19.28	LT	g > 22.3
AT2019dzv-ATLAS19hxm	14:01:45.02 +46:12:56.1	o = 19.23	LT	g > 22.2

Universities for Research in Astronomy (AURA), and the Department of Energy under Contract No. DE-AC02-76SF00515 with the SLAC National Accelerator Laboratory. Additional LSST funding comes from private donations, grants to universities, and in-kind support from LSSTC Institutional Members. E. Bellm is supported in part by the NSF AAG grant 1812779 and grant #2018-0908 from the Heising-Simons Foundation. M. W. Coughlin is supported by the David and Ellen Lee Postdoctoral Fellowship at the California Institute of Technology. Part of this research was carried out at the Jet Propulsion Laboratory, California Institute of Technology, under a contract with the National Aeronautics and Space Administration. D. L. Kaplan was supported by NSF grant AST-1816492. A. K. H. Kong acknowledges support from the Ministry of Science and Technol-

ogy of the Republic of China (Taiwan) under grants 106-2628-M-007-005 and 107-2628-M-007-003. J. S. Bloom and J. Martinez-Palomera are partially supported by a Gordon and Betty Moore Foundation Data-Driven Discovery grant. Harsh Kumar thanks the LSSTC Data Science Fellowship Program, which is funded by LSSTC, NSF Cybertraining Grant #1829740, the Brinson Foundation, and the Moore Foundation; his participation in the program has benefited this work. S. Anand acknowledges support from the PMA Division Medberry Fellowship at the California Institute of Technology. Rahul Biswas, Ariel Goobar and Jesper Sollerman acknowledge support from the G.R.E.A.T research environment funded by the Swedish National Science Foundation. J. Soon acknowledges support by an Australian Government Research Training Program (RTP) Scholarship.

REFERENCES

Aasi et al. 2015, Classical and Quantum Gravity, 32, 074001
 Abbott, B. P., Abbott, R., Abbott, T. D., et al. 2017, Nature, 551, 85
 Abbott, B. P., et al. 2018, arXiv:1811.12907
 Abbott et al. 2017a, Phys. Rev. Lett., 119, 161101. <https://link.aps.org/doi/10.1103/PhysRevLett.119.161101>

—. 2017b, *The Astrophysical Journal Letters*, 848, L13. <http://stacks.iop.org/2041-8205/848/i=2/a=L13>

—. 2017c, *The Astrophysical Journal Letters*, 850, L39. <http://stacks.iop.org/2041-8205/850/i=2/a=L39>

—. 2018, *Living Reviews in Relativity*, 21, 3. <https://doi.org/10.1007/s41114-018-0012-9>

Acernese et al. 2015, *Classical and Quantum Gravity*, 32, 024001

Ahumada, T., Coughlin, M. W., Staats, K., & Dekany, R. G. 2019a, GRB Coordinates Network, Circular Service, No. 24198, #1 (2019/April-0), 24198

Ahumada, T., Coughlin, M. W., Staats, K., et al. 2019b, GCN, 24320

Ahumada, T., Coughlin, M. W., Cenko, S. B., et al. 2018, GRB Coordinates Network, Circular Service, No. 23515, #1 (2018/December-0), 23515

Ahumada, T., Coughlin, M. W., Staats, K., et al. 2019c, GRB Coordinates Network, 24343, 1

Alexander, K. D., Berger, E., Fong, W., et al. 2017, *ApJL*, 848, L21

Anand, S., Kasliwal, M. M., M.W. Coughlin, T. A., et al. 2019, GCN, 24311

Andreoni, I., Anand, S., & Kasliwal, M. 2019a, GRB Coordinates Network, 24349, 1

Andreoni, I., & Bellm, E. 2019, GCN, 24356

Andreoni, I., Cenko, S. B., Masci, F., & Graham, M. 2019b, GCN, 24302

Arcavi, I., Howell, D. A., McCully, C., et al. 2019, GRB Coordinates Network, 24307, 1

Arcavi, I., McCully, C., Hosseinzadeh, G., et al. 2017, *The Astrophysical Journal Letters*, 848, L33. <http://stacks.iop.org/2041-8205/848/i=2/a=L33>

Ascenzi, S., Coughlin, M. W., Dietrich, T., et al. 2019, *Monthly Notices of the Royal Astronomical Society*, 486, 672. <https://doi.org/10.1093/mnras/stz891>

Bauswein, A., Baumgarte, T. W., & Janka, H.-T. 2013, *Phys. Rev. Lett.*, 111, 131101. <https://link.aps.org/doi/10.1103/PhysRevLett.111.131101>

Bauswein et al. 2017, *The Astrophysical Journal Letters*, 850, L34. <http://stacks.iop.org/2041-8205/850/i=2/a=L34>

Bellm, E. C., Kulkarni, S. R., Graham, M. J., et al. 2018, *Publications of the Astronomical Society of the Pacific*, 131, 018002. <https://doi.org/10.1088%2F1538-3873%2Faaecbe>

Bhalerao, V., Kasliwal, M., Bhattacharya, D., et al. 2017, *Astrophys. J.*, 845, 152

Bhalerao, V., Kumar, H., Karambelkar, V., et al. 2019, GCN, 24201

Blagorodnova, N., Neill, J. D., Walters, R., et al. 2018, *Publications of the Astronomical Society of the Pacific*, 130, 035003. <http://stacks.iop.org/1538-3873/130/i=985/a=035003>

Bloom, J. S., Zucker, C., Schlafly, E., et al. 2019, GCN, 24337

Breeveld, A. A., Kuin, N. P. M., Marshall, F. E., et al. 2019, GCN, 24296

Buckley, D., Jha, S. W., Cooke, J., & Mogotsi, M. 2019, GCN, 24205

Burke, J., Hiramatsu, D., Arcavi, I., et al. 2019, GRB Coordinates Network, 24206, 1

Carini, R., Izzo, L., Palazzi, E., et al. 2019, GRB Coordinates Network, 24252, 1

Castro-Tirado, A. J., Hu, Y. D., Li, X. Y., et al. 2019, GRB Coordinates Network, 24214, 1

Cenko et al. 2018, GRB Coordinates Network, Circular Service, No. 22969, #1 (2018/July-0), 22969

Chang, S.-W., Wolf, C., Onken, C. A., Luvaal, L., & Scott, S. 2019a, GCN, 24325

Chang, S. W., Wolf, C., Onken, C. A., et al. 2019b, GRB Coordinates Network, 24260, 1

Chatterjee et al. 2019a, GRB Coordinates Network, Circular Service, No. 24141, #1 (2019/April-0), 24141

—. 2019b, GRB Coordinates Network, Circular Service, No. 24237, #1 (2019/April-0), 24237

Chornock et al. 2017, *The Astrophysical Journal Letters*, 848, L19. <http://stacks.iop.org/2041-8205/848/i=2/a=L19>

Cook, D. O., Kasliwal, M. M., Van Sistine, A., et al. 2017, ArXiv e-prints, arXiv:1710.05016

Coughlin, M. W., Anand, S., & Ahumada, T. 2019, GCN, 24223

Coughlin, M. W., Dietrich, T., Margalit, B., & Metzger, B. D. 2018, arXiv e-prints, arXiv:1812.04803

Coughlin, M. W., Tao, D., Chan, M. L., et al. 2018, *Monthly Notices of the Royal Astronomical Society*, 478, 692. <https://dx.doi.org/10.1093/mnras/sty1066>

Coughlin, M. W., Ahumada, T., Cenko, S. B., et al. 2019a, *Publications of the Astronomical Society of the Pacific*, 131, 048001

Coughlin, M. W., Dekany, R. G., Duev, D. A., et al. 2019b, *Monthly Notices of the Royal Astronomical Society*, 485, 1412. <https://doi.org/10.1093/mnras/stz497>

Coughlin et al. 2018a, GRB Coordinates Network, Circular Service, No. 22871, #1 (2018/July-0), 22871

—. 2018b, GRB Coordinates Network, Circular Service, No. 23324, #1 (2018/October-0), 23324

—. 2018c, GRB Coordinates Network, Circular Service, No. 23379, #1 (2018/October-0), 23379

—. 2018d, GRB Coordinates Network, Circular Service, No. 22739, #1 (2018/May-0), 22739

Cowperthwaite, P. S., Berger, E., Villar, V. A., et al. 2017, *ApJL*, 848, L17

Crawford, S. M., Still, M., Schellart, P., et al. 2010, in Society of Photo-Optical Instrumentation Engineers (SPIE) Conference Series, Vol. 7737, Society of Photo-Optical Instrumentation Engineers (SPIE) Conference Series, 25

De, K., Hankins, M., Adams, S. M., et al. 2019, *GCN*, 24306

Dekany, Smith, et al. 2019, Submitted to *PASP*

Dichiara, S., Gatkine, P., Durbak, J., et al. 2019, *GCN*, 24220

Dimitriadis, G., Jones, D. O., Siebert, M. R., et al. 2019, GRB Coordinates Network, 24358, 1

Drout, M. R., Piro, A. L., Shappee, B. J., et al. 2017, *Science*, 358, 1570

Evans, P. A., Cenko, S. B., Kennea, J. A., et al. 2017, *Science*, 358, 1565

Finn, L. S., & Chernoff, D. F. 1993, *Phys. Rev. D*, 47, 2198. <https://link.aps.org/doi/10.1103/PhysRevD.47.2198>

Flaughier, B., Diehl, H. T., Honscheid, K., et al. 2015, *The Astronomical Journal*, 150, 150

Flewelling, H. 2018, in American Astronomical Society Meeting Abstracts, Vol. 231, American Astronomical Society Meeting Abstracts #231, 436.01

Ghosh, S., Chatterjee, D., Kaplan, D. L., Brady, P. R., & Sistine, A. V. 2017, *Publications of the Astronomical Society of the Pacific*, 129, 114503. <https://doi.org/10.1088%2F1538-3873%2Faa884f>

Ghosh et al. 2019, GRB Coordinates Network, Circular Service, No. 24377, #1 (2019/May-0), 24377

Goldstein, A., Veres, P., Burns, E., et al. 2017, *The Astrophysical Journal*, 848, L14

Golkhou, V. Z., Butler, N. R., Strausbaugh, R., et al. 2018, *The Astrophysical Journal*, 857, 81

Graham, M. J., Kulkarni, S. R., Bellm, E. C., et al. 2019, *Publications of the Astronomical Society of the Pacific*, 131, 078001

Haggard, D., Nynka, M., Ruan, J. J., et al. 2017, *ApJL*, 848, L25

Hallinan, G., Corsi, A., Mooley, K. P., et al. 2017, *Science*, 358, 1579

Hiramatsu, D., Arcavi, I., Burke, J., et al. 2019, GRB Coordinates Network, 24194, 1

Hosseinzadeh, G., et al. 2019, arXiv:1905.02186

Hotokezaka, K., Nakar, E., Gottlieb, O., et al. 2018, arXiv:1806.10596

Hu, Y. D., Castro-Tirado, A. J., Li, X. Y., et al. 2019, GRB Coordinates Network, 24324, 1

Im, M., Kim, J., Paek, G. S. H., et al. 2019, GRB Coordinates Network, 24318, 1

Izzo, L., Carini, R., Benetti, S., et al. 2019, GRB Coordinates Network, 24208, 1

Jencson, J., De, K., Anand, S., et al. 2019, *GCN*, 24233

Jonker, P., et al. 2019, *GCN*, 24221

Just, O., Bauswein, A., Pulpillo, R. A., Goriely, S., & Janka, H.-T. 2015, *Monthly Notices of the Royal Astronomical Society*, 448, 541. <http://dx.doi.org/10.1093/mnras/stv009>

Kaiser, N., Burgett, W., Chambers, K., et al. 2010, in SPIE Proceedings, Vol. 7733, *Ground-based and Airborne Telescopes III*, 77330E

Kann, D. A., Thoene, C., Stachie, C., et al. 2019, GRB Coordinates Network, 24459, 1

Kasen, D., Metzger, B., Barnes, J., Quataert, E., & Ramirez-Ruiz, E. 2017, *Nature*, 551, 80 EP. <http://dx.doi.org/10.1038/nature24453>

Kasliwal, M. M., & Nissanke, S. 2014, *The Astrophysical Journal Letters*, 789, L5. <http://stacks.iop.org/2041-8205/789/i=1/a=L5>

Kasliwal, M. M., Cenko, S. B., Singer, L. P., et al. 2016, *The Astrophysical Journal*, 824, L24. <https://doi.org/10.3847%2F2041-8205%2F824%2F2%2F124>

Kasliwal, M. M., Kasen, D., Lau, R. M., et al. 2019, *Monthly Notices of the Royal Astronomical Society: Letters*, <http://oup.prod.sis.lan/mnrasl/advance-article-pdf/doi/10.1093/mnrasl/slz007/27503647/slz007.pdf>. <https://doi.org/10.1093/mnrasl/slz007>

Kasliwal et al. 2017, *Science*, 358, 1559. <http://science.sciencemag.org/content/358/6370/1559>

—. 2019a, *Publications of the Astronomical Society of the Pacific*, 131, 038003

—. 2019b, *GCN*, 24191

Kilpatrick et al. 2017, *Science*, 358, 1583. <http://science.sciencemag.org/content/358/6370/1583>

Kong, A., Tan, H.-J., Yu, P.-C., Ngeow, C.-C., & Ip, W.-H. 2019, *GCN*, 24301

Kostrzewska-Rutkowska, Z., Hodgkin, S., Delgado, A., et al. 2019, *GCN*, 24354

Lattimer, J. M., & Schramm, D. N. 1974, *ApJL*, 192, L145

Li, L.-X., & Paczynski, B. 1998, *The Astrophysical Journal Letters*, 507, L59. <http://stacks.iop.org/1538-4357/507/i=1/a=L59>

Li, W., Leaman, J., Chornock, R., et al. 2011, *MNRAS*, 412, 1441

Ligo Scientific Collaboration, & VIRGO Collaboration. 2019, GRB Coordinates Network, 24228, 1

Lipunov, V., N.Tyurina, Gorbovskoy, E., et al. 2019a, *GCN*, 24326

Lipunov, V., Gorbovskoy, E., Tyurina, N., et al. 2019b, GRB Coordinates Network, 24241, 1

Mahabal, A., Rebbapragada, U., Walters, R., et al. 2019, Publications of the Astronomical Society of the Pacific, 131, 038002

Margutti, R., Berger, E., Fong, W., et al. 2017, ApJL, 848, L20

Masci, F. J., Laher, R. R., Rusholme, B., et al. 2018, Publications of the Astronomical Society of the Pacific, 131, 018003

McBrien, O., Smartt, S., Smith, K. W., et al. 2019, GCN, 24197

McCully, C., Hiramatsu, D., Howell, D. A., et al. 2019, GCN, 24295

—. 2017, ApJL, 848, L32

Mészáros, P., & Rees, M. J. 1998, The Astrophysical Journal Letters, 502, L105. <http://stacks.iop.org/1538-4357/502/i=2/a=L105>

Metzger, B. D. 2017, Living Rev. Rel., 20, 3

Metzger, B. D., Martínez-Pinedo, G., Darbha, S., et al. 2010, Monthly Notices of the Royal Astronomical Society, 406, 2650

Moore, A. M., & Kasliwal, M. M. 2019, Nature Astronomy, 3, 109

Morihana, K., Jian, M., & Nagayama, T. 2019a, GRB Coordinates Network, 24219, 1

—. 2019b, GRB Coordinates Network, 24328, 1

Morokuma, T., Ohta, K., Yoshida, M., et al. 2019, GRB Coordinates Network, 24230, 1

Muthukrishna, D., Narayan, G., Mandel, K. S., Biswas, R., & Hložek, R. 2019, arXiv e-prints, arXiv:1904.00014

Nicholl, M., Cartier, R., Pelisoli, I., et al. 2019, GCN, 24321

Nicholl et al. 2017, The Astrophysical Journal Letters, 848, L18. <http://stacks.iop.org/2041-8205/848/i=2/a=L18>

Nissanke, S., Kasliwal, M., & Georgieva, A. 2013, ApJ, 767, 124. <http://stacks.iop.org/0004-637X/767/i=2/a=124>

Nordin, J., et al. 2019, arXiv:1904.05922

O'Brien, P. 2018, in COSPAR Meeting, Vol. 42, 42nd COSPAR Scientific Assembly, E1.15–18–18

Oke, J. B., & Gunn, J. E. 1982, PASP, 94, 586

Palmese, A., Soares-Santos, M., Santana-Silva, L., et al. 2019, GCN, 24312

Pavana, M., Kiran, B., & G. C. Anupama, V. B. 2019, GCN, 24200

Perley, D. A., & Copperwheat, C. M. 2019, GCN, 24202

Perley, D. A., Copperwheat, C. M., & Taggart, K. L. 2019a, GCN, 24204

—. 2019b, GCN, 24314

—. 2019c, GRB Coordinates Network, 24314, 1

Pian, E., D'Avanzo, P., Benetti, S., et al. 2017, Nature, 551, 67

Piasek, A., Steele, I. A., Bates, S. D., et al. 2014, in Ground-based and Airborne Instrumentation for Astronomy V, Vol. 9147, International Society for Optics and Photonics, 91478H

Radice, D., Perego, A., Zappa, F., & Bernuzzi, S. 2018, The Astrophysical Journal Letters, 852, L29. <http://stacks.iop.org/2041-8205/852/i=2/a=L29>

Rhodes, L., Fender, R., Williams, D., et al. 2019, GRB Coordinates Network, 24226, 1

Richardson, D., III, R. L. J., Wright, J., & Maddox, L. 2014, The Astronomical Journal, 147, 118. <https://doi.org/10.1088%2F0004-6256%2F147%2F5%2F118>

Rigault, M., Neill, J. D., Blagorodnova, N., et al. 2019, arXiv e-prints, arXiv:1902.08526

Roberts, L. F., Kasen, D., Lee, W. H., & Ramirez-Ruiz, E. 2011, The Astrophysical Journal Letters, 736, L21. <http://stacks.iop.org/2041-8205/736/i=1/a=L21>

Roberts, L. F., Lippuner, J., Duez, M. D., et al. 2017, Monthly Notices of the Royal Astronomical Society, 464, 3907. [+http://dx.doi.org/10.1093/mnras/stw2622](http://dx.doi.org/10.1093/mnras/stw2622)

Rosswog, S. 2015, Int. J. Mod. Phys., D24, 1530012

Rosswog, S., Feindt, U., Korobkin, O., et al. 2017, Class. Quant. Grav., 34, 104001

Savchenko, V., Ferrigno, C., Kuulkers, E., et al. 2017, The Astrophysical Journal, 848, L15

Schady, P., Chen, T. W., Schweyer, T., Malesani, D. B., & Bolmer, J. 2019, GRB Coordinates Network, 24229, 1

Shappee, B. J., Prieto, J. L., Grupe, D., et al. 2014, The Astrophysical Journal, 788, 48

Shappee, B. J., Simon, J. D., Drout, M. R., et al. 2017, Science, 358, 1574

Shappee, B. J., Kochanek, C. S., Stanek, K. Z., et al. 2019, GCN, 24313

Shawhan et al. 2010, GRB Coordinates Network, Circular Service, No. 24098, #1 (2019/April-0), 24098

Singer et al. 2013, The Astrophysical Journal Letters, 776, L34. <http://stacks.iop.org/2041-8205/776/i=2/a=L34>

—. 2015, The Astrophysical Journal, 806, 52

—. 2019a, GRB Coordinates Network, Circular Service, No. 24069, #1 (2019/April-0), 24069

—. 2019b, GRB Coordinates Network, Circular Service, No. 24168, #1 (2019/April-0), 24168

—. 2019c, GRB Coordinates Network, Circular Service, No. 24228, #1 (2019/May-0), 24228

Smartt et al. 2017, Nature, 551, 75 EP. <http://dx.doi.org/10.1038/nature24303>

Smith, K. W., Young, D. R., McBrien, O., et al. 2019, GCN, 24210

Smith, M. P., Nordsieck, K. H., Burgh, E. B., et al. 2006, in Proc. SPIE, Vol. 6269, Society of Photo-Optical Instrumentation Engineers (SPIE) Conference Series, 62692A

Steele et al. 2004, The Liverpool Telescope: performance and first results, , , doi:10.1117/12.551456.
<https://doi.org/10.1117/12.551456>

Tachibana & Miller. 2018, Publications of the Astronomical Society of the Pacific, 130, 128001

Tan, H.-J., Yu, P.-C., Kong, A., et al. 2019a, GCN, 24274

Tan, H.-J., Yu, P.-C., Ngeow, C.-C., & Ip, W.-H. 2019b, GCN, 24193

Tanvir, N. R., Gonzalez-Fernandez, C., Levan, A. J., Malesani, D. B., & Evans, P. A. 2019, GRB Coordinates Network, 24334, 1

Tonry, J. L., Denneau, L., Heinze, A. N., et al. 2018, Publications of the Astronomical Society of the Pacific, 130, 064505.
<http://stacks.iop.org/1538-3873/130/i=988/a=064505>

Troja, E., Piro, L., van Eerten, H., et al. 2017, Nature, 551, 71

Troja, E., Watson, A. M., Becerra, R. L., et al. 2019, GRB Coordinates Network, 24335, 1

Utsumi, Y., Tanaka, M., Tominaga, N., et al. 2017, PASJ, 69, 101

Waratkar, G., Kumar, H., Bhalerao, V., Stanzin, J., & Anupama, G. C. 2019, GCN, 24304

West, A. A., Morgan, D. P., Bochanski, J. J., et al. 2011, AJ, 141, 97

Wiersema, K., Levan, A. J., Fraser, M., et al. 2019, GRB Coordinates Network, 24209, 1

Wijers, R. A. M. J., Rees, M. J., & Mszros, P. 1997, Monthly Notices of the Royal Astronomical Society, 288, L51. <http://dx.doi.org/10.1093/mnras/288.4.L51>

Wright, E. L., Eisenhardt, P. R. M., Mainzer, A. K., et al. 2010, The Astronomical Journal, 140, 1868.
<http://stacks.iop.org/1538-3881/140/i=6/a=1868>

Wu, M.-R., Fernández, R., Mart??nez-Pinedo, G., & Metzger, B. D. 2016, Monthly Notices of the Royal Astronomical Society, 463, 2323.
[+http://dx.doi.org/10.1093/mnras/stw2156](http://dx.doi.org/10.1093/mnras/stw2156)